



Mild and Rapid Light-Driven Suzuki-Miyaura Reactions Catalyzed by AuPd Nanoparticles in Water at Room Temperature

Ana Paula Nazar de Souza,^[a] Luiz Phelipe de Souza Tomaso,^[b] Vitor Alexandre S. da Silva,^[b] Gabriel Francisco S. da Silva,^[a] Evelyn C. S. Santos,^[b, c] Eustáquio de S. Baêta,^[d] José Brant de Campos,^[d] Nakédia M. F. Carvalho,^[a] Luiz Fernando B. Malta,^[b] and Jaqueline D. Senra^{*[a]}

Organic reactions carried out in water under mild conditions are state-of-the-art in terms of environmentally benign chemical processes. In this direction, plasmonic catalysis can aid in accomplishing such tasks. In the present work, cyclodextrin-mediated AuPd bimetallic nanoparticles (NPs) were applied in room-temperature aqueous Suzuki-Miyaura reactions aiming at

preparing biaryl products based on fluorene, isatin, benzimidazole and resorcinol, with yields of 77% up to 95%. AuPd NPs were revealed to be a physical mixture of Au and Pd particles circa 20 and 2 nm, respectively, through X-ray diffraction, dynamic light scattering, UV-Vis spectroscopy and transmission electron microscopy analyses.

Introduction

The search for green and safe chemical reaction protocols has become more intensive in the last few years. The increasing regulations concerning the use of flammable, explosive, carcinogenic and ozone-depleting organic solvents are evidence of an urgent and necessary change to protect both health and environment.^[1–4] Since organic solvents constitute about 80% of chemical industrial waste, a reorientation has to occur in all production segments worldwide, from academic up to industrial research and processes.

Reactions in/on water have been flourishing more recently as an important factor for the development of a sustainable

approach in chemical processes. Indeed, the traditional dogma involving the direct correlation between reactants dissolution and high conversions is limited to only some cases. By definition, “on water” reactions are related to catalyst-free chemical processes performed at the interface of water in a heterogeneous medium. In this case, water is responsible for the acceleration of chemical reactions and the reaction can be categorized into three main groups according to the solubility of reactants^[5,6] In contrast, “in water” processes rely on the events that occur using water as a reaction medium in the presence of a catalyst. In a more general sense, catalytic reactions “in water” can be defined from the phase in which the catalyst is in.^[7] Depending on the temperature and pressure (e.g. supercritical conditions, 374 °C, 22.06 MPa) water can form a homogeneous phase and assume the role of a basic catalyst for the preparation of nanostructures under green conditions.^[8]

Cyclodextrins (CDs) are water-soluble oligosaccharides with a unique host–guest chemistry.^[9–11] Most notably, the presence of CDs as additives in chemical reactions can lead to the formation of dynamic supramolecular aggregates in which the energetics are favored by strong interactions promoted by the confined space. The application of CDs as corrosion inhibitor additives,^[12] mass-transfer agents,^[13] chiral inductors,^[14] enzyme mimics^[15] and metallic nanoparticle stabilizers^[16] are known in several chemical processes performed in water. In the last case, studies centered on the combination of nano-systems containing catalytically active noble metals with the potential to absorb light and drive chemical transformations in water have been rapidly increasing in the last years. Nano-systems containing cyclodextrins have properties that integrate good biocompatibility, a stabilizing effect and an adequate size that does not compromise the plasmonic effect.


In this context, bimetallic catalytic systems are interesting platforms in which the composition can be explored and tuned to achieve new opportunities concerning their optical and


[a] A. P. Nazar de Souza, G. F. S. da Silva, Prof. Dr. N. M. F. Carvalho, Prof. Dr. J. D. Senra
Instituto de Química
Universidade do Estado do Rio de Janeiro, Rio de Janeiro, 20550-900 (Brazil)
E-mail: jaqueline.senra@uerj.br


[b] L. P. de Souza Tomaso, V. A. S. da Silva, Dr. E. C. S. Santos, Prof. Dr. L. F. B. Malta
Instituto de Química
Universidade Federal do Rio de Janeiro, Rio de Janeiro, 21941-909 (Brazil)

[c] Dr. E. C. S. Santos
Centro Brasileiro de Pesquisas Físicas
Rio de Janeiro, 22290-180 (Brazil)

[d] Dr. E. de S. Baêta, Prof. Dr. J. Brant de Campos
Departamento de Engenharia Mecânica
Universidade do Estado do Rio de Janeiro, 20940-200 (Brazil)

 Supporting information for this article is available on the WWW under <https://doi.org/10.1002/open.202200177>

 This publication is part of a Special Collection of ChemistryOpen including invited contributions focusing on the multifaceted chemistry of water - H₂O. Please visit chemistryopen.org/collections to view all contributions.

 © 2022 The Authors. Published by Wiley-VCH GmbH. This is an open access article under the terms of the Creative Commons Attribution Non-Commercial NoDerivs License, which permits use and distribution in any medium, provided the original work is properly cited, the use is non-commercial and no modifications or adaptations are made.

electronic properties. For instance, nanoscale optical phenomena have been enabling manipulation of light at the sub-diffraction limit dimension for waveguides^[17] along with reaction acceleration and control of molecular transformations.^[18] Thus, plasmonic nanomaterials pave the way to the comprehension of light-driven efficiency based on both particle morphology and composition.

The preparation of nanoalloys based on Pd has been extensively investigated in the last years since Pd-catalyzed cross-couplings can provide important building blocks for the synthesis of fine chemicals.^[19] These bimetallic systems have been employed to boost the reactivity in comparison to their monometallic counterparts. In general, their catalytic activity has a strong dependence on the charge transfer between both metals depending on their nature, for instance, if they are of core-shell or eutectic-like structures.^[20] Since the work by Reetz and co-workers with active Pd/Ni alloys for Suzuki-Miyaura reaction,^[21] several other examples followed. Synthetic strategies are usually carried out with the controlled nucleation-growth of the metal precursors by using selected reducing and stabilizing agents (such as ascorbic acid^[22,23] and/or surfactant(s), such as CTAC^[24] and PVP^[25]).

Taking advantage of the gold-palladium alloy miscibility,^[20,23] catalytic systems based on a photophysical activation can have pronounced activities because of the integration between the strong light-absorbing plasmonic Au nanoparticles and the catalytically active Pd sites.

Indeed, bimetallic AuPd NPs are of relevance because of the possibility of harvesting light energy by tuning the size, shape and atomic ratio of those particles, properties which are

primarily involved in the energetic electron transfer. Thus, the localized surface plasmon (LSP) effect, thoroughly reviewed in the literature,^[26] can result in enhanced catalytic activity. Different works have shown the potential of AuPd NPs in the Suzuki-Miyaura coupling, exploring visible light irradiation.^[24,27–30]

In this work, we aimed to synthesize Au–Pd bimetallic nanoparticles under different conditions by using the citrate-cyclodextrin method. The catalytic system was explored in Suzuki-Miyaura reactions in neat water under visible light irradiation at room temperature. The goal was to take advantage of the gold nanoparticles towards visible light excitation in order to achieve higher product yields in energy-efficient and simple conditions.

Results and Discussion

The X-ray powder diffractograms of the Au, Pd and AuPd nanoparticles, with a zoomed-in inset for the main reflection, are shown in Figure 1a. The monometallic Au and Pd nanoparticles crystallize in a face-centered cubic (fcc) lattice (JCPDS cards n. 04-0784 and 88-2335 for Au and Pd, respectively) with the (111) peaks located at 38.21° and 40.08°, respectively, while bimetallic nanoparticles showed peaks at 38.28° and 38.38° (lyophilized and deposited bimetallic nanoparticles, respectively). This result led to the assignment of the (111) peak of the bimetallic nanoparticles as belonging to the fcc structure of gold, hence not exhibiting significant signs of alloying. The decrease in intensity of the reflection peak observed for AuPd in comparison to Au without significant displacement suggests

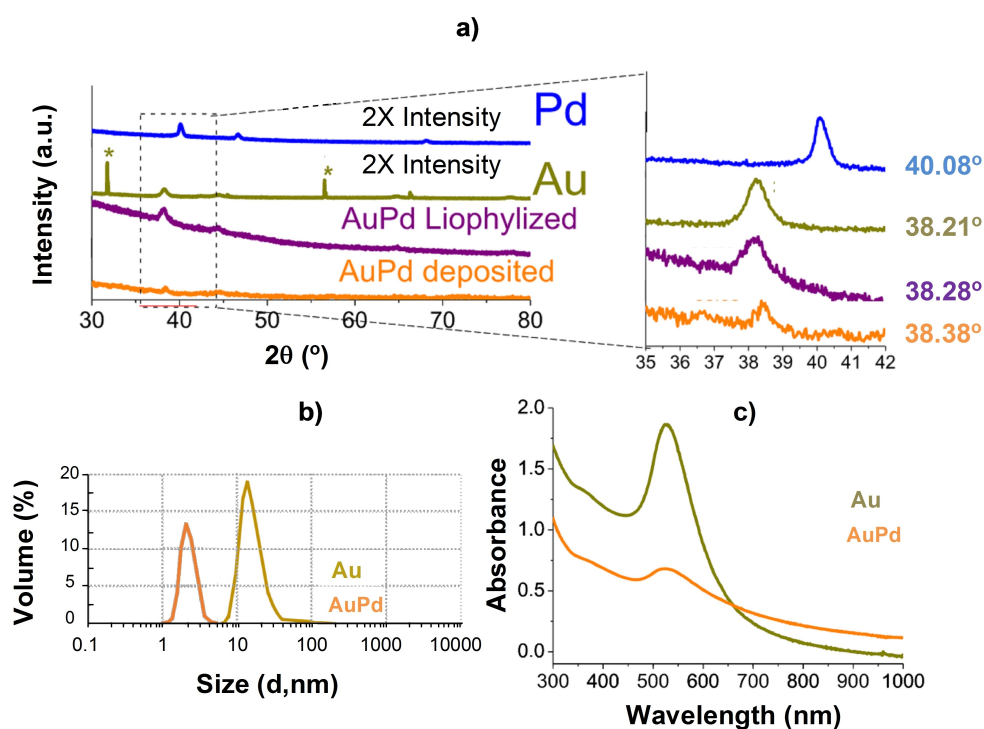


Figure 1. a) Powder X-ray diffractograms for Pd, Au, and AuPd NPs with zoomed-in region relating to the (111) reflection. Peaks marked with asterisks are attributed to a NaCl phase; b) Dynamic light scattering curves for Au and AuPd NPs dispersions; c) UV-Vis spectra for Au and AuPd NPs dispersions.

core-shell morphology formation.^[31] Moreover, the absence of the Pd (111) reflection for the bimetallic XRD patterns could be attributed to the metal forming a thin shell around the gold nanoparticles, below the detection limit of the technique.^[32] Potentially, the palladium nanoparticles were so small that no X-ray diffraction and interference occurred significantly. This latter case would indicate a physical mixture between Au and Pd NPs.

In order to investigate the size of the bimetallic nanoparticles, colloidal dispersions of Au and AuPd nanoparticles were studied by dynamic light scattering (DLS). As shown in Figure 1b, both dispersions were characterized by a unimodal particle size distribution with maxima at 2.2 and 16.3 nm for the AuPd and Au nanoparticles, respectively, that is, the bimetallic nanoparticles were smaller than the Au nanoparticles. The smaller hydrodynamic diameter of the bimetallic nanoparticles would indicate the effect of core-shell morphology on the size as well as the important role of β -HPCD in stabilizing the nanoparticles and avoiding agglomeration, as demonstrated in previous work of our group.^[16] More importantly, almost the entire volume (99.9%) of the bimetallic nanoparticles dispersion relates to sizes around 2 nm (0.1% of volume relate to particles of circa 30.9 nm), which allows inferring that these NPs were so small that nearly no diffraction and interference of X-rays would occur on the crystallites of these particles hence producing low-intensity, wide peaks or even no peaks in the XRD patterns, as observed in Figure 1a.

The optical properties of gold nanoparticles are well known.^[33–35] In order to investigate these properties, the as-prepared nanoparticles were studied by UV-Vis absorption spectroscopy (Figure 1c). The gold nanoparticles show maximum absorption at 524 nm assigned as the localized surface plasmon resonance (LSPR). In comparison, the AuPd nanoparticles show the LSPR band at the same region, however, with lower intensity. The decrease in intensity of the LSPR band could be related to the core-shell formation,^[35] and to the decrease of the particle size,^[36,37] a phenomenon that also impacts the absorption energy.

Figure 2 shows the TEM images of the AuPd bimetallic nanoparticles. Clearly, it is possible to see that the nanostructured system is predominantly characterized by a bimodal distribution. The characterization studies unambiguously show that the larger particles consisted of monometallic arrays. In addition, the presence of bimetallic nanoparticles was not so clear, but they appeared to be smaller and more disperse than Au nanoparticles (Figure 2a and Figure S1, Supporting Information, respectively) which agreed with the UV-Vis spectroscopy discussion (Figure 1c). This could result from the imposed metallic mixture and/or cyclodextrin-induced better stabilization of Au and Pd particles. Some nanoparticles up to 20 nm (Figure 2d) were selected for electron diffraction (Figure 2f) and EDS analysis (Figure 2g–h). However, these particles constituted the minor volumetric part in the bimetallic suspension, as revealed by DLS analysis (Figure 1b), and they were basically formed from Au (Figure 2f, g and h) although residual palladium was found on their surfaces (Figure 2h). Bearing in mind that Au and Pd were employed in a 1:1 molar ratio, the major part of

palladium was assumed to form NPs with minor size distribution. Closely examining the background of the TEM images shown in Figures 2b–c, tiny nanoparticles were found (Figures 2c and 2e). The size distribution histogram (inset of Figure 2c) evidenced particles around 2 nm which agreed with the DLS results for the AuPd bimetallic suspension (Figure 1b). To structurally identify such particles, the interplanar distances were obtained at $d(111)=2.23$ Å and $d(200)=1.98$ Å, in contrast to $d(111)=2.30$ Å and $d(200)=2.00$ Å for Au (Figure 2d), hence allowing identifying them as the palladium nanoparticles. The explanation for such small Pd nanoparticles is the presence of cyclodextrin in significant molar excess (1:50), enabling steric stabilization;^[7] Au nanoparticles in their turn seems to be mainly stabilized by electrosteric stabilization of citrate anions, according to the zeta potential measurements (-18.0 and -18.1 mV for Au and AuPd, respectively). Therefore, alloying and core-shell processes did not seem to be the ways of constituting these bimetallic nanoparticles; instead, the bimetallic suspension can be described as a physical mixture of bigger particles around 20 nm almost entirely constituted of Au; and of smaller particles around 2 nm constituted of Pd.

Table 1 summarizes the results of the catalytic tests under (or without) irradiation by using monometallic and bimetallic NPs in the Suzuki-Miyaura reaction between 4-bromoacetophenone and phenylboronic acid, which was chosen as a model. For the reaction, Au NPs and Pd NPs were first catalytically evaluated in control experiments in water under light irradiation. The reactions presented in Table 1 were carried out in the presence of light and were carefully maintained at the same temperature as the reactions conducted in the dark at 25 ± 1 °C. The relative contributions of light irradiation to the catalytic conversions were obtained by subtracting conversions in the dark from conversions under irradiation. The irradiation was kept with a light intensity of 1.0 W cm⁻².

As observed in Table 1, entry 1, the reactions with the Au NPs did not show any activity, regardless of the ambient light conditions. Even at a higher temperature (70 °C), no product was formed (Table 1, entry 2). However, the Pd NPs system showed adequate conversions (Table 1, entry 3) which were also independent of lighting. Conversely, catalytic performance of the bimetallic AuPd system proved sensitive to ambient light (Table 1, entry 4): yields were higher in the presence of light, indicating a possible synergy between the bimetallic system and visible light. Indeed, we also tested the Au: Pd 2:1 ratio of the AuPd NPs for the catalytic activity evaluation in the dark and under light irradiation. As shown in Table 1, entry 5 was similar to that one obtained with a 1:1 Au: Pd ratio. For comparison, the bimetallic system combined with TiO₂ – a well-known photocatalyst with an absorption spectrum predominantly in the UV region^[39–41] – afforded outstanding catalytic results, even at only 1 h of reaction time (Table 1, entry 6). A similar increase in product yield was obtained for Pd NPs + TiO₂ (Table 1, entry 7). As a control experiment, when TiO₂ or Au NPs/TiO₂ were tested, no product was observed (Table 1, entries 8 and 9), as expected in the absence of an active catalytic site. Under light irradiation, both exhibit higher conversion efficiencies. Even though the Au: Pd ratio can

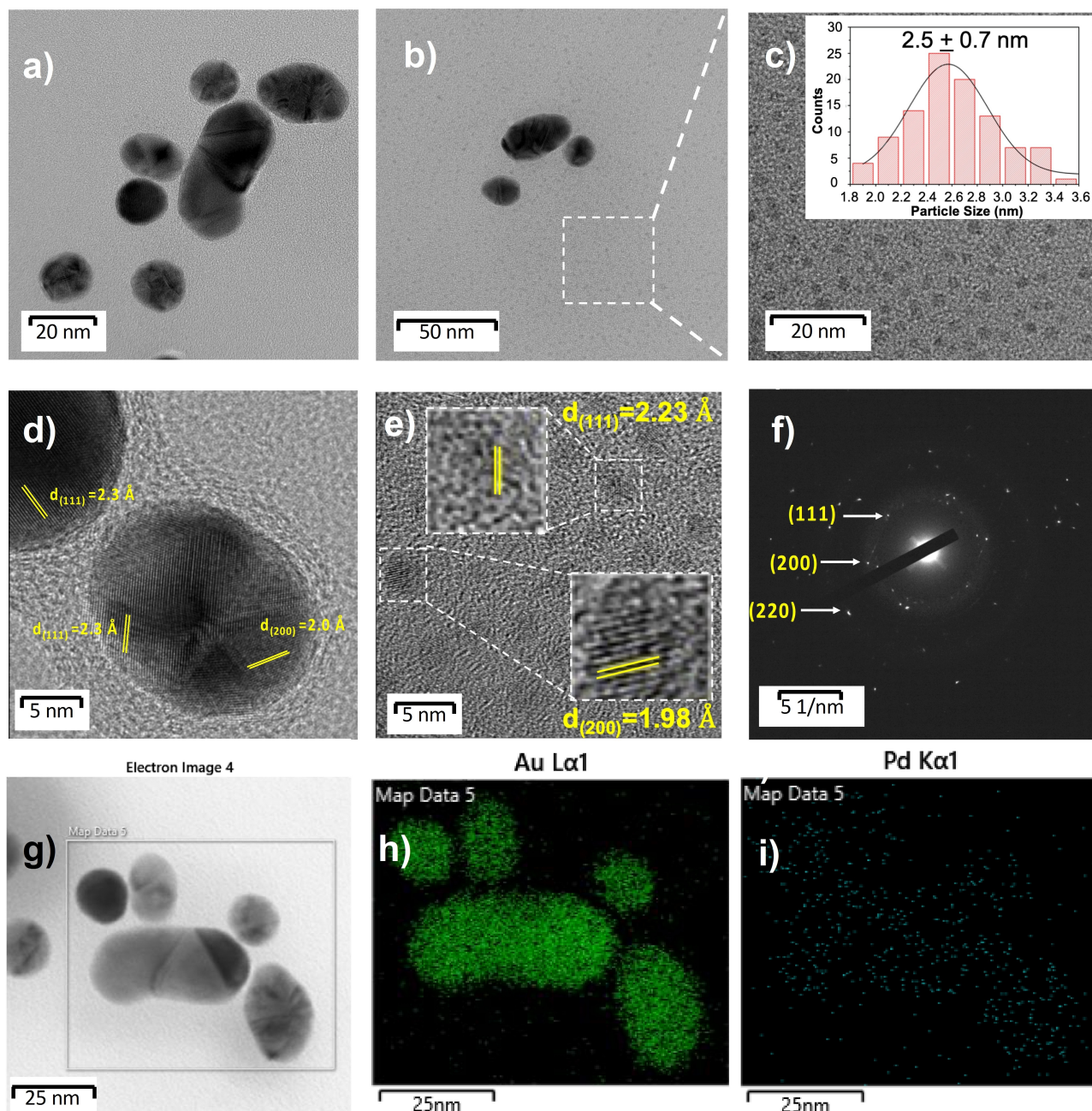



Figure 2. TEM (a–c) and HRTEM (d,e) images of AuPd bimetallic nanoparticles in the presence of hydroxypropylated β -cyclodextrin; The inset in (c) represents the histogram with the particle size distribution of the smallest nanoparticles; d-spacing of bimetallic AuPd (d) and the corresponding SAED image (f). Electron micrograph region of AuPd NPs (g) and EDS elemental mapping showing the presence of Au (h) and Pd (i), represented as green and cyan dots, respectively.

strongly influence the charge heterogeneity of the cluster, it is possible that the adsorption rate of the substrate was not significantly affected (Table 1, entry 10). The effect of other inorganic bases proved to be almost identical (Table 1, entries 11 and 12) in comparison with the best result with pure AuPd NPs (Table 1, entry 4).

As observed, the light irradiation significantly improved the catalytic activity of the AuPd NPs when compared to dark conditions. The dependence of the catalytic conversion with the light is probably due to the LSPR effect, which can be responsible of transferring energy to the reaction and promot-

ing a photocatalytic effect. The contribution of the light irradiation was calculated through the differences between the yield under light and under dark at the same temperature (25 °C). For instance, the reaction conversion in Table 1, entry 4 revealed that 27% conversion can be attributed to light irradiation. Interestingly, the use of the AuPd NPs with higher Au content did not lead to a remarkable increase in the light contribution (Table 1, entry 9), as expected considering, that the LSPR of gold is exclusively in the visible spectrum. In addition, TON values demonstrated a good reaction efficiency profile up to 870 by using the pure bimetallic catalytic system. A blank

Table 1. Catalytic survey applying 4-bromoacetophenone and phenylboronic acid as substrates for light-activated Suzuki-Miyaura reaction.^[a]


Entry	Catalyst [mol %]	Yield [%]		TON		Contribution of light irradiation [%]
		Dark	Light	Dark	Light	
1	Au NPs (0.1 mol %)	< 5	< 5	< 50	< 50	–
2	Au NPs (0.1 mol %)	0 ^[b]	0 ^[b]	0	0	–
3	Pd NPs (0.1 mol %)	60	61	600	610	1
4	AuPd NPs (1:1, Au: Pd) (0.1 mol % Pd)	60	87	600	870	27
5	AuPd NPs (2:1, Au: Pd) (0.1 mol % Pd)	49	84	490	790	35
6	AuPd NPs + TiO ₂ (1:1, Au: Pd) (0.1 mol % Pd)	80 60 ^[c]	99 80 ^[c]	800 600 ^[c]	990800 ^[c]	19 20 ^[c]
7	Pd NPs + TiO ₂ (0.1 mol %)	60 48 ^[c]	99 77 ^[c]	600 480 ^[c]	990 770 ^[c]	39 29 ^[c]
8	Au NPs + TiO ₂ (1 mol %)	–	< 5	–	< 50	–
9	TiO ₂ ^[c]	0	0	0	0	–
10	AuPd NPs + TiO ₂ ^[c] (2:1, Au: Pd) (0.1 mol % Pd)	49	88	490	880	39
11	AuPd NPs (1:1, Au: Pd) (0.1 mol % Pd) ^[d]	56	75	560	750	19
12	AuPd NPs (1:1, Au: Pd) (0.1 mol % Pd) ^[e]	51	69	510	690	18


[a] 0.25 mmol 4-bromoacetophenone, 0.25 mmol phenylboronic acid, 0.5 mmol K₂CO₃, 3.55 mL H₂O, 1 mol % Pd, 25 °C, 2 h. Yields were obtained from GC-MS. [b] Reaction temperature = 70 °C. [c] Reaction time = 1 h. [d] 0.5 mmol Cs₂CO₃. [e] 0.5 mmol Na₃PO₄.

experiment containing only the reagents - without the catalyst - was carried out under the same reaction conditions described in Table 1, entry 4. However, no conversion was detected for 4-bromoacetophenone. Furthermore, the AuPd catalyst was submitted to the reaction conditions of entry 4 (Table 1) with and without light irradiation. These two sets of nanoparticles were visualized by SEM-FEG and TEM (Figures S2 and S3, respectively) and were compared to the original AuPd nanoparticles. AuNPs sizes between 17.3 ± 1.2 nm and 27.3 ± 1.3 nm

were found for both samples with no distinguishable size range and morphologies among them. Indeed, the TEM images (Figure S3) evidenced a uniform particle size distribution for the Au NPs and Pd NPs, the last ones between 2.0–3.5 ± 0.1 nm. Therefore, the reaction conditions were not deleterious to the AuPd nanoparticles' size and morphologies.

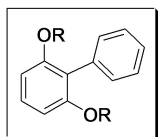
For the reaction between 4-chloronitrobenzene and phenylboronic acid, low to ordinary yields were obtained since this aryl halide is less activated for the oxidative addition step of the Suzuki-Miyaura catalytic cycle. The Pd NP system afforded a low yield even under lighting (< 5%, Table 2, entry 1). No conversion was observed for the pure Au NPs (Table 2, entry 2). In contrast, the bimetallic system led to an increase from 7% to 30% when irradiated with visible light (Table 2, entry 3). However, the combination with TiO₂ was detrimental, probably related to a possible partial photodecomposition by virtue of the presence of the NO₂ group (Table 2, entry 4).

The catalytic system was evaluated by applying other aryl bromides to better understand the contributions of light irradiation to the reaction efficiencies and selectivities in some deactivated substrates (Scheme 1) such as resorcinol, isatin, fluorene and benzimidazole cores. Such arylated derivatives have applications in the field of medicinal chemistry and organic electronics.^[42–47] Substrates were predominantly non-polar, which, however, did not constitute in itself a problem for the catalytic outcome since conversions up to 95% were obtained in neat water at 25 °C. In this case, the presence of cyclodextrins (CDs) in the catalytic system - which are known phase transfer agents - could be responsible for increasing the good catalytic results in light of the supramolecular complexes formed. In this case, CDs can lead to some differences in activation energies.^[48] Concerning reaction selectivities, the

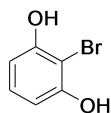
Table 2. Suzuki-Miyaura reaction with 4-chloronitrobenzene and phenylboronic acid.^[a]


Entry	Catalyst [mol %]	Yield [%]	
		Dark	Light
1	PdNPs (0.1 mol %)	< 5	< 5
2	AuNPs (1.0 mol %)	–	–
3	AuPdNPs (1:1, Au: Pd) (0.1 mol % Pd)	7	30
4	AuPdNPs/TiO ₂ (1:1, Au: Pd) (0.1 mol % Pd)	7	9
5	TiO ₂	–	–

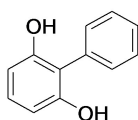
[a] 0.25 mmol 4-bromoacetophenone, 0.25 mmol phenylboronic acid, 0.5 mmol K₂CO₃, 3.55 mL H₂O, 1 mol % Pd, 25 °C, 2 h. Yields were obtained from GC-MS.

Substrate class: resorcinol

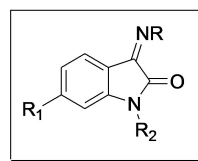
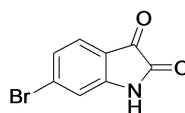
Biological applications

Reductive elimination from pincer Co^{III} complex (2020)

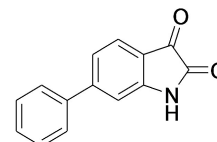
2-bromoresorcinol



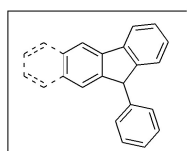
2-phenylresorcinol

61% (light, 2 h)
83% (light, 70 °C, 24 h)*Substrate class: isatin*Biological/ photovoltaic
applications

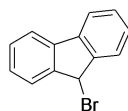
6-bromoisatin



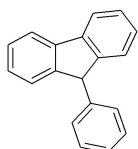
6-phenylisatin

84 % (light, 25 °C, 1 h)
87% (light, 25 °C, 24 h)*Substrate class: fluorene*Biological/ photovoltaic
applications

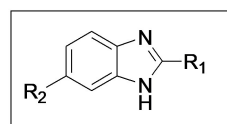
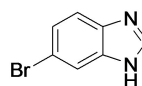
Radical cascade (2015)



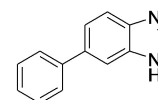
9-H-9'-bromofluorene



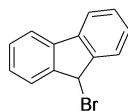
9-H-9'-phenylfluorene

92% (light, 25 °C, 2 h)
95% (light, 25 °C, 24 h)Biological/ photovoltaic
applications

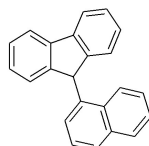
6-bromoimidazole



6-phenylimidazole

77 % (light, 25 °C, 2 h)
81% (light, 25 °C, 24 h)

9-H-9-bromofluorene



9-H-9-naphthylfluorene

79 % (light, 25 °C, 2 h)
83 % (light, 25 °C, 24 h)

Scheme 1. Class-oriented Suzuki-Miyaura reactions with aryl bromides and arylboronic acid catalyzed by AuPd NPs in neat water. Conditions: 0.25–1.0 mmol aryl bromide, 0.25–1.0 mmol phenylboronic acid, 0.5–2.0 mmol K₂CO₃, 3.55–14.2 mL H₂O, 0.1 mol % Pd, T(°C), t(h).

formation of side products was not observed. Interestingly, the reaction with resorcinol exhibited a moderate to good catalytic

result, in spite of the steric hindrance caused by the 1,3-dihydroxyl substituents. Nicely, the increase in temperature

improved the catalytic conversion to a yield above of 80%. Results involving the use of more hydrophobic 9H-9-bromofluorene also indicated a good conversion in the presence of phenyl and naphthyl boronic acids, even in the absence of hydrogen-bond acceptor sites. Reactions with nitrogenated heterocycles were carried out under the same conditions. Nicely, we also observed high conversions, even when using benzimidazole, which can impart some deactivation to the catalytic first step. The presence of the isatin core related to the electron-withdrawing effect demonstrated to activate the reaction in 1 h. A detrimental use of cyclodextrins cannot be ruled out: although these macrocycles act as phase transfer agents, the partial complexation of some substrates can slow down some reactions.

Conclusion

Here, the combined effects of light activation and Au/Pd bimetallic catalytic sites produced good to excellent catalytic results for the preparation of biaryls in mild conditions, namely in water and at room temperature. Following the best catalytic conditions (0.1 mol% Pd), yields up to 95% for aryl bromides containing fluorene, resorcinol, benzimidazole and isatin cores were obtained in the presence of ambient light. This turns out to be a promising result since only 2 h as reaction times were generally sufficient in each case. However, catalytic tests with 4-nitrochlorobenzene – a less activated aryl chloride – led to only a moderate yield of 30%.

The AuPd bimetallic nanoparticles were revealed to be a physical mixture that has a concerted modus operandi in the Suzuki-Miyaura reactions. The ~20 nm Au particles conceivably constituted the antenna-like part of the system: in this case, it can allow an energy transfer to the ~2 nm Pd particles, which can then better catalyze reactions under these simple and green conditions. Even the particles' stabilization differed between Pd and Au: while the former NPs were maintained metastable by steric effects of cyclodextrin stabilization, the latter particles were suspended by electrosteric effects due to citrate adsorption, since the zeta potential measured for bimetallic suspension and monometallic Au colloid were the same (−18.0 mV). The role of cyclodextrin role can be a matter of discussion since the hydroxypropylated form can certainly reduce and stabilize Pd but no such significant conclusions could be drawn for the structuration of the bimetallic Au/Pd system. There is evidence that cyclodextrin can act as an additive to modulate the shape and size of Au nanoparticles. On the other hand, the activity of cyclodextrin in great molar excess may inhibit a core-shell structuration between the metal sites. This is currently the subject of ongoing studies in our research group.

Experimental Section

Materials

All reactions were performed under air using adequate glassware with controlled bath temperature. All chemicals were purchased at the highest commercial grade and used as received. Analytical thin-layer chromatography (TLC) was performed using E. Merck silica gel 60 F254 pre-coated glass plates (0.25 mm-thickness). For every solution prepared in this method, distilled water was used as solvent.

Preparation of the catalyst

The Au–Pd hybrid nanoparticles were synthesized through a two-step process, starting by the synthesis of the gold nanoparticles (Au NPs). For this preparation, 2.5 mL of 4 mM NaAuCl₄·2H₂O solution were diluted to a final volume of 11.25 mL. The resulting solution was heated, while magnetically stirred, in an oil bath, until refluxing started. After reflux, 1.0 mL of 40 mM sodium citrate dihydrate solution were added dropwise. The reaction proceeded under reflux for 30 min. For the second step, 0.5 mL of 5 mM Na₂PdCl₄ solution were added to 3.05 mL of the AuNPs suspension previously prepared. The mixture was heated, while magnetically stirred, in an oil bath, to 80 °C. Then, 172.5 mg of 2-hydroxypropyl-β-cyclodextrin (β-HPCD) were added (1 Pd: 50 β-HPCD, molar ratio). The reaction proceeded at 80 °C for 30 min.

Catalyst characterization

The nano-analysis of the particles was performed by transmission electron microscopy (TEM) using a JEOL 2100F microscope (LABNANO/CBPF), operated at an accelerating voltage of 200 kV. The sample was deposited on a carbon film supported by 400 mesh copper grids. The images were obtained in TEM and HRTEM mode with a CCD camera (OneView Orius, 16 Mpixel) and in scanning mode (STEM). Compositional maps were obtained by energy-dispersive X-ray spectroscopy (EDS) using a beam spot size of 1 nm. The particle size distribution was obtained from TEM images by measuring the diameter of about two hundred particles using ImageJ software.

The nano equipment ZS90 from LAMATE, UFF was used to measure the zeta potential. For each analysis, the dilution of samples in ultrapure water in the proportion of 0.5:3 was used. The samples were analyzed with the number of measurements on automatic, angle of 90° with spread set at 173° and temperature at 25 °C, allowing 1 min of temperature stabilization before measurements, 10 runs of 10 s each were made.

To measure the average particle size of the aqueous dispersions, dynamic light scattering (DLS) was performed with a Zetasizer nano S90 (Malvern). Data were analyzed using the equipment software (ZetaSizer 10.11.1, Malvern). The data obtained refer to the mean ± standard deviation of the mean.

UV-Vis electronic spectroscopy analysis was conducted in an Agilent 8453 diode array spectrophotometer (USA). Spectra were acquired for solutions in quartz cuvettes with 1.0 cm optical path in the 200–900 nm interval. This analysis was also performed to assess the stability of the nanoparticles for months.

XRD diffractograms with 2θ ranging from 10° to 80° were collected using the X'Pert PRO diffractometer (Philips, Panalytical). Voltage of 40 kV and current of 40 mA, angular step of 0.026° and step time of 1000 s were used. The measurements were carried out supported by a glass and placed inside the sample holder.

Catalytic survey

The correspondent NPs dispersion (Au NPs, Pd NPs or AuPd NPs) were used in a 0.25 mmol scale of aryl halide (4-bromoacetophenone or 4-chloronitrobenzene), 0.25 mmol of phenylboronic acid and 0.50 mmol of base (K_2CO_3 or $Na_3PO_4 \cdot 12 H_2O$). The reactions were carried out in a round-bottom flask without a heating source. The control tests were performed inside a black box so as to avoid contact with light. The main reactions were exposed to a light source (halogen lamp) with a intensity of $1.0 W cm^{-2}$, 500 W, under temperature control. All reactions were isolated by liquid-liquid extraction using $3 \times 5 mL$ of a dichloromethane/ethyl acetate mixture (1:1). 1H and ^{13}C NMR spectra were recorded on a Bruker AV-500 spectrometer at 25 °C. Chemical shift values are reported in δ (ppm) downfield from tetramethylsilane with reference to internal residual solvent ($CDCl_3$). Coupling constants (J) are reported in hertz (Hz). Multiplicities of signals are designated as follows: s=singlet; d=doublet; t=triplet; m=multiplet; br=broad. High-resolution mass spectra (HRMS) were obtained on a Bruker microTOF II mass spectrometer using ESI as the source type.

Supporting Information Summary

Additional TEM and SEM-FEG images of AuPdNPs as well as 1H and ^{13}C NMR spectra of all catalytic products can be found in the Supporting Information.

Acknowledgements

The authors acknowledge CAPES, FAPERJ and CNPq for the financial support. J. D. Senra in particular would like to thank CNPq for Universal project process 422656/2018-6 and FAPERJ APQ1 project process SEI-260003/001693/2021. L.F.B. Malta in his turn would like to thank for funding from FAPERJ Jovem Cientista do Nosso Estado process E-26/203.212/2017; and N. M. F. Carvalho would like to thank FAPERJ for the Apoio à Infraestrutura e Pesquisa nas Universidades Estaduais do Rio de Janeiro – 2021, project SEI-260003/014203/2021. We also thank the Multiuser Laboratory of Nanoscience and Nanotechnology (LABNANO) from CBPF.

Conflict of Interest

The authors declare no conflict of interest.

Data Availability Statement

Research data are not shared.

Keywords: water · biaryl · Au nanoparticles · Pd nanoparticles · plasmonic catalysis

[1] A. T. Sutton, K. Fraige, G. M. Leme, V. da Silva Bolzani, E. F. Hilder, A. J. Cavalheiro, R. D. Arrua, C. S. Funari, *Anal. Bioanal. Chem.* **2018**, *410*, 3705–3713.

- [2] S. Khandelwal, Y. K. Tailor, M. Kumar, *J. Mol. Liq.* **2016**, *215*, 345–386.
[3] N. A. Isley, F. Gallou, B. H. Lipshutz, *J. Am. Chem. Soc.* **2013**, *135*, 17707–17710.
[4] L. Peng, Z. Hu, Q. Lu, Z. Tang, Y. Jiao, X. Xu, *Chin. Chem. Lett.* **2019**, *30*, 2151–2156.
[5] R. N. Butler, A. G. Coyne, *Org. Biomol. Chem.* **2016**, *14*, 9945–9960.
[6] R. N. Butler, A. G. Coyne, *Chem. Rev.* **2010**, *110*, 6302–6337.
[7] T. Kitanosono, S. Kobayashi, *Chem. Eur. J.* **2020**, *26*, 9408–9429.
[8] A. A. Raheem, P. Thangasamy, M. Sathish, C. Praveen, *Nanoscale Adv.* **2019**, *1*, 3177–3191.
[9] W. Zhan, T. Wei, Q. Yu, H. Chen, *ACS Appl. Mater. Interfaces* **2018**, *10*, 36585–36601.
[10] J. Wankar, N. G. Kotla, S. Gera, S. Rasala, A. Pandit, Y. A. Rochev, *Adv. Funct. Mater.* **2020**, *30*, 1909049.
[11] B. Yang, J. Lin, Y. Chen, Y. Liu, *Bioorg. Med. Chem.* **2009**, *17*, 6311–6317.
[12] T. M. de Souza, R. F. Cordeiro, G. M. Viana, L. C. Aguiar, L. F. de Senna, L. F. B. Malta, E. D'Elia, *J. Mol. Struct.* **2016**, *1125*, 331–339.
[13] J. D. Senra, L. F. B. Malta, L. C. S. Aguiar, A. B. C. Simas, O. A. C. Antunes, *Curr. Org. Chem.* **2010**, *14*, 1337–1355.
[14] L. F. B. Malta, Y. Cordeiro, L. W. Tinoco, C. C. Campos, M. E. Medeiros, O. A. C. Antunes, *Tetrahedron: Asymmetry* **2008**, *19*, 1182–1188.
[15] L. Wang, X. Qu, Y. Xie, S. Lv, *Catalysts* **2017**, *7*, 289.
[16] J. D. Senra, L. F. B. Malta, R. C. Michel, Y. Cordeiro, R. A. Simao, A. B. Simas, L. C. Aguiar, *J. Mater. Chem.* **2011**, *21*, 13516–13523.
[17] S. A. Maier, H. A. Atwater, *J. Appl. Phys.* **2005**, *98*, 10.
[18] N. Motl, A. Smith, C. DeSantis, S. Skrabalak, *Chem. Soc. Rev.* **2014**, *43*, 3823–3834.
[19] A. F. Biajoli, C. S. Schwalm, J. Limberger, T. S. Claudino, A. L. Monteiro, *J. Braz. Chem. Soc.* **2014**, *25*, 2186–2214.
[20] R. Ferrando, J. Jellinek, R. L. Johnston, *Chem. Rev.* **2008**, *108*, 845–910.
[21] M. T. Reetz, R. Breinbauer, K. Wanninger, *Tetrahedron Lett.* **1996**, *37*, 4499–4502.
[22] L. Srisombat, J. Nonkumwong, K. Suwannarat, B. Kuntalue, S. Ananta, *Colloids Surf. A Physicochem. Eng. Asp.* **2017**, *512*, 17–25.
[23] X. Zhu, Q. Guo, Y. Sun, S. Chen, J.-Q. Wang, M. Wu, W. Fu, Y. Tang, X. Duan, D. Chen, Y. Wan, *Nat. Commun.* **2019**, *10*, 1428.
[24] M. K. Gangishetty, A. M. Fontes, M. Malta, T. L. Kelly, R. W. Scott, *RSC Adv.* **2017**, *7*, 40218–40226.
[25] Y. Xiang, X. Peng, X. Kong, Z. Tang, H. Quan, *Colloids Surf. A Physicochem. Eng. Asp.* **2020**, *594*, 124652.
[26] G. Baffou, R. Quidant, *Chem. Soc. Rev.* **2014**, *43*, 3898–3907.
[27] D. Han, Z. Bao, H. Xing, Y. Yang, Q. Ren, Z. Zhang, *Nanoscale* **2017**, *9*, 6026–6032.
[28] N. A. Nemygina, L. Z. Nikoshvili, I. Y. Tiamina, A. V. Bykov, I. S. Smirnov, T. LaGrange, Z. Kaszkur, V. G. Matveeva, E. M. Sulman, L. Kiwi-Minsker, *Org. Process Res. Dev.* **2018**, *22*, 1606–1613.
[29] S. Rohani, A. Ziarati, G. M. Ziarani, A. Badii, T. Burgi, *Catal. Sci. Technol.* **2019**, *9*, 3820–3827.
[30] P. Verma, Y. Kuwahara, K. Mori, H. Yamashita, *J. Mater. Chem. A* **2016**, *4*, 10142–10150.
[31] P. Gnanaprakasam, A. Gowrisankar, S. Senthilkumar, A. Murugadoss, T. Selvaraju, R. V. Mangalaraja, *Mater. Sci. Eng. B* **2021**, *264*, 114924.
[32] E. Westsson, G. J. Koper, *Catalysts* **2014**, *4*, 375.
[33] P. Ghosh, V. Thambi, A. Kar, A. L. Chakraborty, S. Khatua, *Optics Lett.* **2021**, *46*, 4562–4565.
[34] K. Chang, S. Wang, H. Zhang, Q. Guo, X. Hu, Z. Lin, H. Sun, M. Jiang, J. Hu, *PLoS One* **2017**, *12*, e0177131.
[35] A. G. Al-Rubaye, A. Nabok, A. Tsargorodska, *Sens. Bio-Sens. Res.* **2017**, *12*, 30–35.
[36] J. G. Ruiz-Montoya, L. M. Nunes, A. M. Baena-Moncada, G. Tremiliosi-Filho, J. C. Morales-Gomero, *Int. J. Hydrogen Energy* **2021**, *46*, 23670–23681.
[37] J. Piella, N. G. Bastus, V. Puentes, *Chem. Mater.* **2016**, *28*, 1066–1075.
[38] D. García-Lojo, S. Núñez-Sánchez, S. Gomez-Grana, M. Grzelczak, I. Pastoriza-Santos, J. Pérez-Juste, L. M. Liz-Marzán, *Acc. Chem. Res.* **2019**, *52*, 1855–1864.
[39] Z. Shayegan, C.-S. Lee, F. Haghighat, *Chem. Eng. J.* **2018**, *334*, 2408–2439.
[40] R. Hazime, Q. Nguyen, C. Ferronato, A. Salvador, F. Jaber, J.-M. Chovelon, *Appl. Catal. B* **2014**, *144*, 286–291.
[41] A. Fernandes, M. Gagol, P. Makoś, J. A. Khan, G. Boczkaj, *Sep. Purif. Technol.* **2019**, *224*, 1–14.
[42] S. Ullah, S. Son, H. Y. Yun, D. H. Kim, P. Chun, H. R. Moon, *Expert Opin. Ther. Pat.* **2016**, 347–362.

- [43] B. J. Foley, C. M. Palit, S. D. Timpa, O. V. Ozerov, *Organometallics* **2018**, *37*, 3803–3812.
- [44] L.-H. Xie, S.-H. Yang, J.-Y. Lin, M.-D. Yi, W. Huang, *Phil. Trans. R. Soc. A* **2013**, *371*, 20120337.
- [45] K. Pati, G. P. dos Passos Gomes, T. Harris, A. Hughes, H. Phan, T. Banerjee, K. Hanson, I. V. Alabugin, *J. Am. Chem. Soc.* **2015**, *137*, 1165–1180.
- [46] Varun, Sonam, R. Kakkar, *MedChemComm* **2019**, *10*, 351–368.
- [47] P. Sharma, C. LaRosa, J. Antwi, R. Govindarajan, K. A. Werbovets, *Molecules* **2021**, *26*, 4213.
- [48] C. Gaeta, P. La Manna, M. De Rosa, A. Soriente, C. Talotta, P. Neri, *ChemCatChem* **2021**, *13*, 1638–1658.

Manuscript received: August 7, 2022

Revised manuscript received: October 30, 2022
